Suspended-core fibres as optical gas sensing cells: study and implementation

Isabelle Dicaire, Jean-Charles Beugnot, and Luc Thévenaz

Swiss Federal Institute of Technology, École Polytechnique Fédérale de Lausanne (EPFL), Institute of Electrical Engineering, Station 11, 1015 Lausanne, Switzerland

ABSTRACT

We have thoroughly studied and modelled many important aspects for the realization of gas-light interactions in suspended-core fibres. The fraction of the optical field propagating in holes could be calculated from the fibre geometry to predict the total absorption for a given molecular absorption line and fibre length. In addition, the gas diffusion into the fibre holes could be modelled to precisely anticipate the filling time for a given fibre geometry and length. This was experimentally validated by preparing several samples of suspended-core fibres showing various lengths. These samples were filled with acetylene at low pressure (< 50 mbar) and were hermetically and permanently sealed by fusion splicing each fibre end to a plain single-mode silica fibre. The adequacy between the modelling and the experimental results turned out to be excellent. Several physical parameters essential for the fibre characterization could be extracted from a set of measurements, sketching a specific metrological approach dedicated to this type of fibre. Finally, applications and advanced experiments that can be specifically carried out using these fibres are discussed.

Keywords: Fiber optics sensors, microstructure devices, absorption, evanescent field sensor, diffusion, photonic crystal fibres, detection.

1. INTRODUCTION

Photonic crystal fibres (PCF) are now widely used to study the interaction between light and matter. The high interaction length achievable in such small volumes provides efficient gas sensing capabilities. More specifically, hollow-core (HC) PCFs are the most efficient fibres with respect to the percentage of light propagating in the sensing volume. Their guiding mechanism based on a photonic bandgap structure allows a nearly total overlap between the optical field and the gas species. However, the transmission in these fibres is subject to any variation in the microstructure, limiting the transmission bandwith to ∼150nm and increasing the fabrication costs.[1] In addition, HC-PCFs can simultaneously propagate several optical modes and their interference is detrimental for many applications. Hollow-core fibres are also difficult to splice to standard silica fibres due to the high sensitivity of the thin silica web to temperature. When successfully spliced, they present substantial Fresnel reflections as a result of the large index difference between the two fibre cores.

Given those limitations, suspended-core fibres (SCFs) based on evanescent-field spectroscopy are good candidates for studying light-matter interactions. Their standard guiding mechanism provides robustness, easy fabrication as well as wide transmission bandwidths[2] and can compensate for the significant reduction of optical power propagating in the sensing volume. The power fraction can nevertheless be increased up to 29% by lowering the core diameter to 0.8μm for an operating wavelength of $\lambda = 1550$ nm.[3] Two important consequences are that single-mode propagation will be secured for this diameter but strong splicing challenges will arise. Even if a compromise diameter can be found and a fibre be drawn, one has to measure this power fraction to quantify the sensitivity of the sensing device. The structure of the propagated modes is then crucial in evaluating this power fraction and for this purpose numerical simulations can be very helpful. From the fibre geometry, we could calculate the fraction of the optical field propagating in the cladding holes and compare it with the value obtained from experiments.

Once the optical properties of the suspended-core fibre are found, the fibre can be filled with a gas species to make gas-light interactions. Even if some studies on the gas filling process have been conducted, they mainly

Correspondence should be addressed to isabelle.dicaire@epfl.ch

Photonic Crystal Fibers III, edited by Kyriacos Kalli, Proc. of SPIE Vol. 7357
73570U · © 2009 SPIE · CCC code: 0277-786X/09/$18 · doi: 10.1117/12.820791

concern analysis of the diffusion process of one gas species in air[4] or in nitrogen.[5] The filling process was usually performed at atmospheric pressure in small cladding holes, therefore the effect of the viscous flow was not taken into account when fitting the experimental data.[6] The theory behind this curve fitting was explored by Henningsen and Hald (2008) in hollow-core fibres, including description of the free molecular flow and the viscous flow, but the combined effect of both types of flow was not characterized.[7] In all cases, the filling process of pure gas in empty SCFs was not studied. In this paper, the filling process of low-pressure acetylene gas in SCFs is both theoretically and experimentally studied. We will see that the hydrodynamic flow must be taken into account due to the sufficiently large diameter of the cladding holes. Thanks to the theory of gaseous flow through capillaries, we could calculate the theoretical diffusion coefficient as a function of pressure and evaluate the effect of changing the cladding hole diameter.

This was experimentally validated by filling several samples of SCFs with low-pressure (<50 mbar) acetylene gas. Using different fibre lengths, we could model the gas diffusion inside the SCF to precisely anticipate the filling time for a given hole diameter and fibre length. In addition, experimental diffusion coefficients were obtained from curve fitting the filling process and good agreements with theoretical values were obtained. Once the samples were filled, they were hermetically and permanently sealed by fusion splicing each fibre end to a plain single-mode silica fibre. The splicing technique should avoid air contamination of the sample and should maximize the coupling of light through the suspended core. Once spliced, the power fraction in air could be experimentally determined from the observed absorption for a given molecular line and compared to the value obtained from calculations. Studies of the transmission output were also conducted to investigate the origin of interference patterns observable as a function of wavelength. Using the various fibre lengths, we could find that the oscillating pattern could be identified as an interference between two guided modes in the fibre core, namely the fundamental optical mode and the first-order degenerated optical mode. This sketches a specific metrological approach dedicated to this type of fibre. Finally, applications and advanced experiments that can be specifically carried out using these fibres are discussed.

2. OPTICAL PROPERTIES

The suspended-core fibre that was used in the experiments was modelled to obtain its optical properties. This typical all-silica SCF shows a 1.2μm core diameter surrounded by three large cladding holes with diameters of 15 μm. Numerical simulations of the optical modes propagating in such fibre have been done using the Matlab toolbox called *Source model technique package (SMTP)*.[8] The structure of the fundamental and first-order modes is illustrated in Figures 1 and 2 respectively. The colour scale indicates the distribution of the z component of the Poynting vector S_z across the fibre. From the Poynting vector S_z, the fraction Φ of the optical power propagating

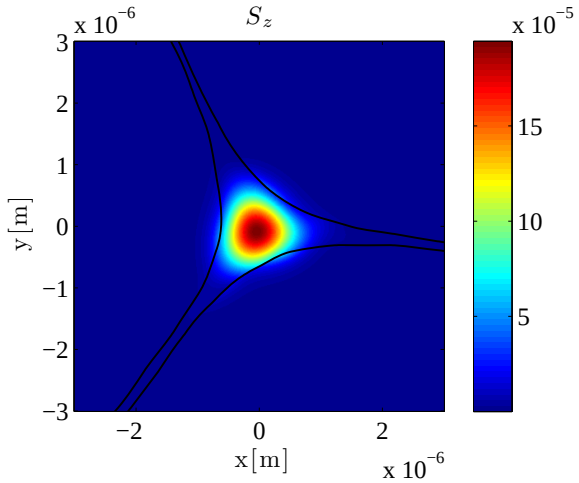

Figure 1. Power distribution of the fundamental mode, $n_{\text{eff}} = 1.314$.

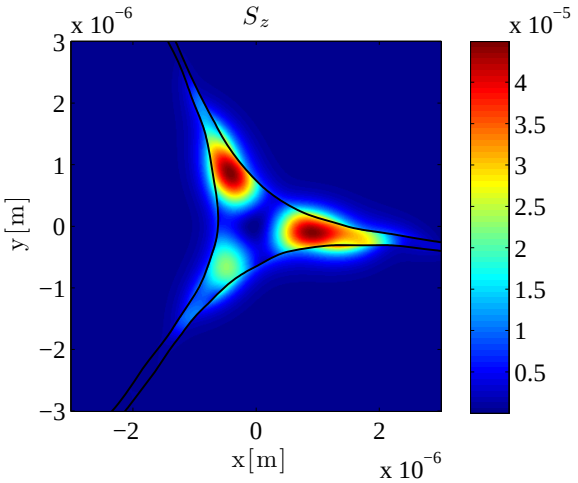

Figure 2. Power distribution of the first-order mode, $n_{\text{eff}} = 1.245$.

in the cladding holes could be calculated:

$$\Phi = \frac{\int_{holes} \mathbf{Re}(S_z)\, dx\, dy}{\int_{total} \mathbf{Re}(S_z)\, dx\, dy} \times 100 = \frac{\int_{holes} \mathbf{Re}(E_x H_y^* - E_y H_x^*)\, dx\, dy}{\int_{total} \mathbf{Re}(E_x H_y^* - E_y H_x^*)\, dx\, dy} \times 100, \quad (1)$$

where $E_{x/y}$ is the electrical field in the x or y direction and $H_{x/y}$ is the magnetic field in the x or y direction.

Using this equation, the theoretical power fraction is 12.6% for the fundamental mode. The effective refractive indices of $n_{\text{eff},1} = 1.314$ and $n_{\text{eff},2} = 1.245$ were obtained for the fundamental and first-order mode, respectively. As calculated, the difference in effective indices is 0.07. All these optical parameters will be helpful to interpret the results shown hereafter.

3. GAS FILLING DYNAMICS

Studies of the filling process of acetylene gas in SCFs were also conducted to better characterize these fibres. According to the theory of flow of gases through tubes,[9] three different flow regimes can be identified. This partition is generally realized using the Knudsen number K_n, which is the ratio of the mean free path λ of a molecule to the radius a of a cylindrical tube through which the gas is flowing:

$$\lambda = \frac{1}{\sqrt{2}\pi N \delta^2} = \frac{k_B T}{\sqrt{2}\pi \bar{P} \delta^2}\ ,\ K_n = \lambda / a, \quad (2)$$

where N is the average volume density of molecules, $\bar{P}$ is the average pressure inside the tube, and δ is the diameter of the acetylene molecule (334 pm).[7] Small Knudsen numbers ($K_n < 0.01$) indicates that collisions between molecules occur more frequently than with the fibre walls, meaning that large holes or high filling pressures are present. In this situation, the flow velocity profile is parabolic across the fibre holes and tends to be zero at the fibre walls due to frictional forces. The gas flow is then considered viscous and is governed by hydrodynamical equations. More specifically, the Poiseuille equation describes the total volume per second F that flows through one cladding hole and turns out to be a fourth power of the hole radius:

$$F_v = \frac{\pi a^4}{8\eta L} \bar{P}, \quad (3)$$

where η is the viscosity and L is the cladding hole length. From the volumetric flow rate F, one can obtain the diffusion coefficient D:

$$D_v = \frac{FL}{\pi a^2} = \frac{a^2 \bar{P}}{8\eta}. \quad (4)$$

On the other hand, large Knudsen numbers ($K_n > 1$) indicates small holes or low-pressure filling of gas and one has to evaluate the effect of wall collisions on the free path of molecules. Since there are few molecular collisions, this flow range is called free-molecular flow (or simply molecular flow) and is pressure-independent. According to Knudsen's work, the volumetric flow rate F and the diffusion coefficient D are:

$$F_K = \frac{2\pi a^3}{3L} \bar{v}\ ,\ D_K = \frac{2}{3} a \bar{v}, \quad (5)$$

where the mean molecular velocity $\bar{v}$ is function of both temperature T and molecular mass m:

$$\bar{v} = \sqrt{\frac{8 k_B T}{\pi m}}, \quad (6)$$

Between the two flow ranges, a transition region is found were both types of collisions influence the characteristics of the flow. As illustrated in Figure 3, the extrapolation of the viscous flow curve (the black dashed line) into the transition region underestimates the actual volumetric flow. The additional flow can be seen as gas slipping over the fibre walls: the flow velocity there is not zero. There are no analytical expressions describing the so-called slip-flow transition region, so we had to rely on semi-empirical relations.

As a result of a series of measurements, Knudsen developped an empirical relation giving the volumetric flow rate in the slip-flow regime based on the Knudsen number K_n scaling the additional flow:

$$F = F_v + Z(K_n)F_K, \tag{7}$$

where $Z(K_n)$ is function of the average pressure inside the cladding hole $\bar{P}$, the hole radius a, the temperature T, and the viscosity η of the gas. Knudsen's expression for Z is:

$$Z = \frac{1 + 2\frac{a}{\eta}\sqrt{\frac{m}{K_B T}}\bar{P}}{1 + 2.47\frac{a}{\eta}\sqrt{\frac{m}{K_B T}}\bar{P}}, \tag{8}$$

but with the help of the kinetic-theory relation for the viscosity:

$$\eta = 0.499\rho\bar{v}L, \tag{9}$$

one can obtain a simplified version of Z, now only depending on the Knudsen number K_n and valid for all gaseous species:

$$Z = \frac{1 + 2.507(a/\lambda)}{1 + 3.095(a/\lambda)} = \frac{1 + 2.507/K_n}{1 + 3.095/K_n}. \tag{10}$$

This way, at low pressure values, Z equals unity and the pressure-dependent flow F_v goes to zero, therefore the volumetric flow is given by the Knudsen equation F_K(Eq. 5) as we enter the molecular regime. On the opposite, as the pressure value increases, the viscous flow F_v increases and the additional flow becomes negligible.

By using the same equation form as in Eq. 7 but for diffusion coefficients, one can obtain the theoretical diffusion coefficient in the slip-flow regime. Figure 4 presents the theoretical diffusion coefficient in suspended-core fibres as a function of pressure for two given hole diameters. The speed of the filling process is improved by increasing the hole diameter or by increasing the operating pressure. Figure 4 also shows that the correction for viscous flow is not significant for small cladding holes, in agreement with Hoo et al. (2003).[6] For an average pressure of 50 mbar inside the fibre holes and a 15μm hole size, a theoretical diffusion coefficient of 33 cm^2/s is calculated. In the next section, we will compare this theoretical value with the one obtained from measurements.

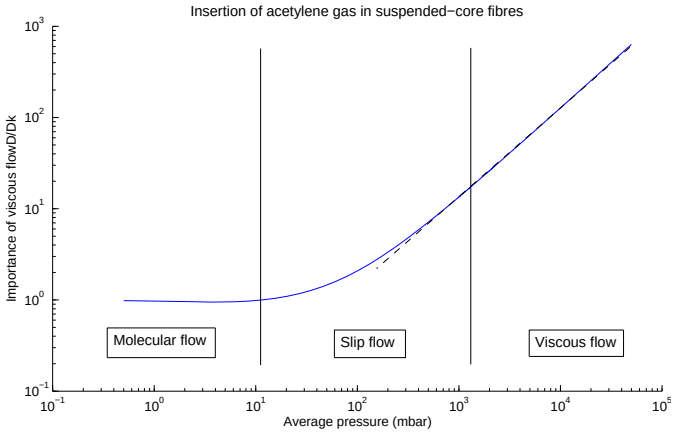

Figure 3. Different flow regimes according to pressure

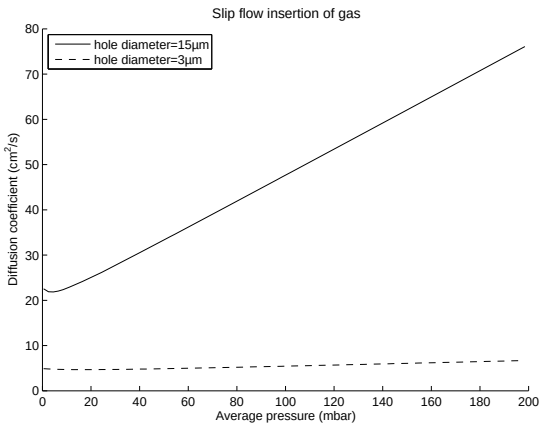

Figure 4. Diffusion coefficient

4. ACETYLENE GAS EXPERIMENTS

4.1 Acetylene loading

Several samples of SCFs showing different lengths were filled with acetylene gas. The fibres were first spliced to a standard single-mode fibre (SMF) at one end using a FSM-40S Fujikura arc fusion splicer. A dispersion-compensating fibre (DCF) showing a $\sim 4\mu$m core size was spliced between the two fibres to better match the

mode field diameters. Splicing losses of 1dB were obtained between the standard fibres and 3–4dB losses between the SCF and the DCF. Once the SCF was successfully spliced at one end, it was placed inside a gas chamber and vacuum was maintained for 4–7 days to let air evacuate the cladding holes. It is crucial to completely evacuate air from the fibre since any residual air with substantially broaden the absorption line and bias the filling procedure. Acetylene gas was then introduced inside the chamber at a pressure of 50 mbar. This target pressure was selected as for higher pressure values collisions between molecules start to broaden the minimum linewidth given by the Doppler broadening (∼500 MHz). Narrow absorption lines give precise wavelength references which are key devices for metrological applications.[10]

The filling process was then monitored using the P14 absorption line at $\lambda = 1533.46$nm. The modulation current of a distributed-feedback (DFB) laser was adjusted to make the laser line sweep across the acetylene line with a repetition rate of 5 Hz and a burleigh WA-1000 wavemeter was used to obtain wavelength information. Figure 5 presents the decrease in relative transmission as a function of time for a 6m long fibre. Knowing the physical length of the sample, we could fit the filling curve to retrieve the experimental diffusion coefficient:

$$I = I_0 \exp\{-\Phi\alpha L(1 - \frac{8}{\pi^2} \sum_{j=1,3,\ldots}^{\infty} \frac{1}{j^2} \exp[-(\frac{j\pi}{2L})^2 Dt])\}. \quad (11)$$

A diffusion coefficient of $30 \pm 1\,\mathrm{cm}^2/\mathrm{s}$ was obtained experimentally, therefore in agreement with the theoretical value of 33 cm^2/s. The small difference can be explained by some air molecules still remaining inside the fibre, which would slightly slow down the filling process. As one can see from Figure 4, the molecular-flow regime can not accurately predict the diffusion coefficient since a value of 23 cm^2/s was expected for 15μm holes. The viscous flow must therefore be taken into account due to the large diameter of the cladding holes.

The same filling procedure was carried out for three different samples and filling times were retrieved for each fibre length. The filling time was defined as the time required for the average pressure to reach 99% of the introduced pressure. The black dots in Figure 6 presents the experimental filling time for each sample. The model[11] approximates Eq. 11 for sufficiently large times t:

$$t_{fill} = \frac{(\xi L)^2}{\pi^2 D} \ln[\frac{\pi^2}{8} \times \frac{P_{in} - \bar{P}}{P_{in}}], \quad (12)$$

where the parameter ξ is a correcting factor taking into account the filling setup and equals 2 in our case. Filling a fibre from one end is equivalent to filling from both sides a fibre whose length is twice longer. The diffusion coefficient obtained using this approximate equation gives $D = 37\mathrm{cm}^2/\mathrm{s}$, in agreement with our previous results. The filling time for a 3μm hole size was also predicted using the filling model with the appropriate theoretical diffusion coefficient and the result is shown in Figure 6 as a dashed line. We could therefore model the gas diffusion inside the SCF to precisely anticipate the filling time for a given hole diameter and fibre length.

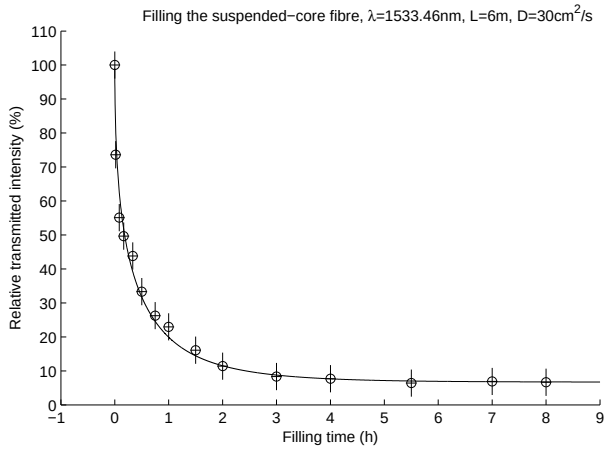

Figure 5. Acetylene loading in 6m long SCF.

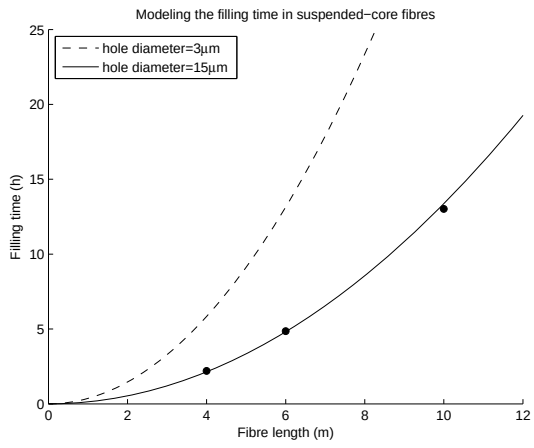

Figure 6. Experimental filling time vs fibre length

4.2 All-fibre gas cell

Once the samples were filled with acetylene, they were hermetically and permanently sealed to make an all-fibre gas cell using the splicing scheme presented in section 4.1. One technical challenge was to splice at atmospheric pressure a low-pressure filled fibre while preventing air from contaminating the sample. We used for this purpose the fibre cell fabrication technique presented by Light, Couny, and Benabid (2006)[12] and based on helium diffusion through silica. Once successfully spliced, the transmission spectrum of the all-fibre acetylene gas cells could be obtained using an optical spectrum analyzer (OSA) and an erbium-doped fibre amplifier (EDFA) as the broadband source (see Figure 8).

Individual absorption lines were also measured over a narrower wavelength range using the setup presented in section 4.1. Figure 7 illustrates the P15 acetylene line where an average pressure of 63 mbar was introduced inside the 10m-long fibre. By calculating the number density N corresponding to this pressure thanks to the ideal gas law, the transmitted intensity through 10m of absorbing media was estimated using Eq. 11 for a filled fibre and where $\alpha = 0.013\,\mathrm{cm}^{-1}$ was theoretically computed as $\alpha = S_\lambda N$. By comparing with the observed absorption, we could experimentally determine the power fraction in the cladding holes to $\Phi = 13 \pm 1\%$. This experimental value is in close agreement with the theoretical value $\Phi = 12.6\%$ obtained from numerical simulations.

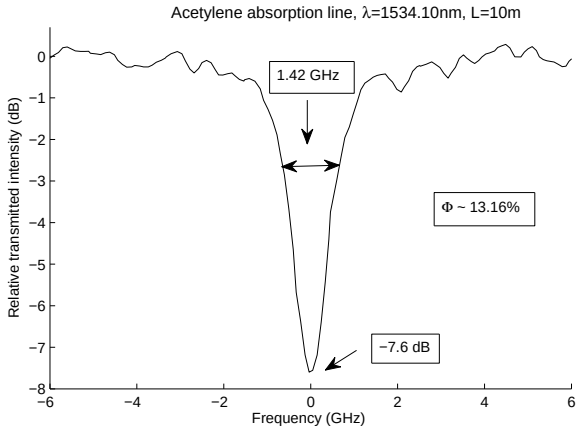

Figure 7. P15 absorption line obtained in a SCF gas cell.

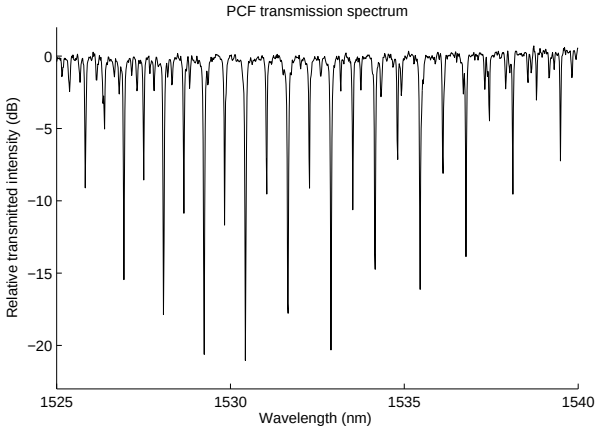

Figure 8. Typical transmission spectrum of SCF gas cell

4.3 Implementation issues

This section will discuss some issues that may rise when working with SCFs. For example, Figure 7 shows an absorption line that is far from being Doppler-limited, although only 63 mbar of $^{12}C_2H_2$ were present in the fibre holes. This deviation is due to the fact that some air was remaining inside the cladding holes before acetylene loading. It can be quite difficult to completely evacuate air from the cladding holes of a long fibre since the diffusion time is a quadratic function of the filling length.

This same Figure also illustrates the background noise that is often seen in PCF spectra. In hollow-core PCFs, this inherent noise is believed to be due to surface modes[13] or polarization properties and the positioning of the fibre.[14] However, we believe there is another origin for SCFs. Studies of the interference pattern in different fibres samples were conducted to investigate its possible origin. The interference pattern was more defined for short fibre lengths and the oscillation period Δf was larger. We could identify the oscillating pattern as an interference between two propagated modes whose effective refractive index difference is:[15]

$$\Delta n_{\mathrm{eff}} = \frac{c}{L\Delta f}. \tag{13}$$

Figure 9 presents Δn_{eff} as a function of fibre length where the error bars take into account the uncertainty on the oscillation period, wavelength, and fibre length. The difference in effective indices is independent of the fibre length, indicating that the interference pattern is due to the intrinsic properties of the suspended-core

fibre. The two optical modes are separated by a value $\Delta n_{\text{eff}} = 0.08$, compatible with an interference between the fundamental optical mode and the first-order degenerated optical mode. Recalling the numerical simulation in section 2 where the effective index difference between theses modes was calculated to be 0.07, this strongly support the assumption that the multimode nature of SCFs is the origin of the interference pattern. This limitation can however be a good motivation for finding an evanescent-field fibre geometry showing single-mode behaviour and high power fraction in the cladding holes while being robust enough to avoid strong splicing and cleaving issues.

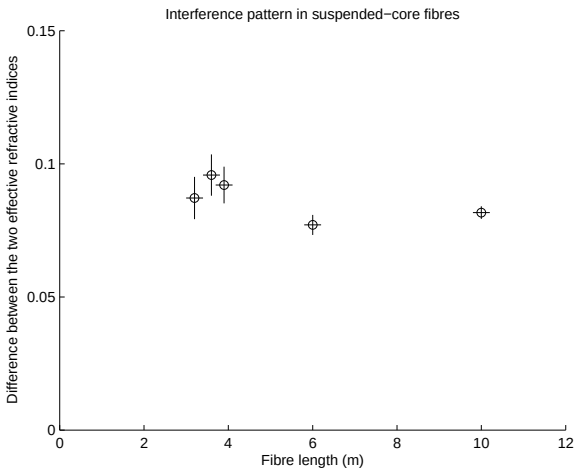

Figure 9. Study of the interference pattern in the transmission output of SCFs.

5. APPLICATIONS

The all-fibre transportable gas cells have many applications in various domains such as laser stabilization and gas-based nonlinear optics. It can be used in a frequency stabilization unit to increase the wavelength accuracy and stability of lasers. This is usually achieved by locking the laser frequency to different absorption lines using C_2H_2 bulk cells[16] for the 1.5μm range. Since Doppler-limited lines show 472 MHz linewidths, saturated absorption lines can be seen as a major improvement due to their 2 MHz linewidth spectral features. In this technique, a counterpropagating pump beam is launched inside the fibre with an optical power higher than the saturation power in order to pump at least 1/4 of the ground-state molecules into the excited state (Bennett hole). The low-power probe beam propagating inside the fibre will experience partial transparency of the medium for a defined Doppler frequency corresponding to the same velocity seen by the two counterpropagating beams. For other frequencies, the two beams will interact with completely different molecules and the absorption line will show the usual Doppler profile. The width of the resulting central dip in the absorption profile is then function of all other broadening sources but Doppler. This central dip, sometimes called Lamb dip, was observed in hollow-core fibres containing low-pressure acetylene gas[13,17] . The measured full width of the Lamb dip was $\sim$40 MHz in both cases and varied with input pump power, gas pressure, and diameter of the gas cell. The difference from the expected 2 MHz width turned out to be explainable by both the transit time broadening and the wall collision broadening in hollow-core fibres.

The all-fibre gas cell can also be used to study light-matter interactions. For instance, the possibility of enhancing Beer-Lambert absorption with slow light was recently theoretically demonstrated in liquid-infiltrated photonic crystals.[18] The experimental confirmation of this effect would be quite interesting for optical gas detection in microsystems. Efficient nonlinear interactions between light and matter can also be realized thanks to the small core size of SCFs which enhances the light intensity. By filling nonlinear material inside the cladding holes, the effective nonlinearity can further be increased. Experiments such as stimulated Raman scattering can then be performed with high efficiency in gas-filled suspended-core fibres.

6. CONCLUSION

Suspended-core fibres (SCFs) are gaining more attention as gas probing devices due to their standard guiding mechanism and the high optical power that is propagating in the cladding holes. This paper presents a theoretical study of the filling process of a gas species in empty SCFs to predict the filling time for a given fibre length and hole size. Several fibre lengths were filled with low-pressure acetylene gas and were permently sealed to plain silica fibres. Experiments were then conducted to retrieve important physical properties of the fibre. The high performances of these fibres suggest that the splicing challenges inherent to the 0.8μm air-suspended core-size fibre should be overcome to reach single-mode propagation as well as high power fractions in the sensing volume.

ACKNOWLEDGMENTS

We thank University Marie-Curie Skłodowskiej, Lublin for providing the suspended-core fibres in the framework of COST 299 Action "FIDES". This work is financially supported by the European Space Agency (ESA) through Grant No. 20200/06/NL/PA and by the Swiss National Office for Education and Research through Project COST C06.0015.

REFERENCES

[1] Benabid, F., "Hollow-core photonic bandgap fibre: new light guidance for new science and technology," *Philosophical Transactions of the Royal Society A: Mathematical, Physical and Engineering Sciences* **364**(1849), 3439–3462 (2006).

[2] Euser, T. G., Chen, J. S. Y., Scharrer, M., Russell, P. S. J., Farrer, N. J., and Sadler, P. J., "Quantitative broadband chemical sensing in air-suspended solid-core fibers," *Journal of Applied Physics* **103**(10), 103108 (2008).

[3] Webb, A. S., Poletti, F., Richardson, D. J., and Sahu, J. K., "Suspended-core holey fiber for evanescent-field sensing," *Optical Engineering* **46**(1), 010503 (2007).

[4] Zhi-guo, Z., Fang-di, Z., Min, Z., and Pei-da, Y., "Gas sensing properties of index-guided PCF with air-core," *Optics Laser Technology* **40**, 167–174 (Feb. 2008).

[5] Gayraud, N., Kornaszewski, Ł. W., Stone, J. M., Knight, J. C., Reid, D. T., Hand, D. P., and MacPherson, W. N., "Mid-infrared gas sensing using a photonic bandgap fiber," *Appl. Opt.* **47**(9), 1269–1277 (2008).

[6] Hoo, Y. L., Jin, W., Shi, C., Ho, H. L., Wang, D. N., and Ruan, S. C., "Design and modeling of a photonic crystal fiber gas sensor," *Appl. Opt.* **42**(18), 3509–3515 (2003).

[7] Henningsen, J. and Hald, J., "Dynamics of gas flow in hollow core photonic bandgap fibers," *Appl. Opt.* **47**(15), 2790–2797 (2008).

[8] Hochman, A. and Leviatan, Y., "Efficient and spurious-free integral-equation-based optical waveguide mode solver," *Opt. Express* **15**(22), 14431–14453 (2007).

[9] Dushman, S., of General Electric Research Laboratory, J. M. L. R. S., and Brown, S. C., "Scientific foundations of vacuum technique," *American Journal of Physics* **30**(8), 612–612 (1962).

[10] Benabid, F., Couny, F., Knight, J. C., Birks, T. A., and Russell, P. S. J., "Compact, stable and efficient all-fibre gas cells using hollow-core photonic crystal fibres," *Nature* **434**, 488–491 (2005).

[11] Jost, W., [*Diffusion in solids, liquids, gases*], Academic Press, New York :, 3rd printing with addendum. ed. (1970).

[12] Light, P. S., Couny, F., and Benabid, F., "Low optical insertion-loss and vacuum-pressure all-fiber acetylene cell based on hollow-core photonic crystal fiber," *Opt. Lett.* **31**(17), 2538–2540 (2006).

[13] Henningsen, J., Hald, J., and Peterson, J. C., "Saturated absorption in acetylene and hydrogen cyanide in hollow-core photonic bandgap fibers," *Opt. Express* **13**(26), 10475–10482 (2005).

[14] Ritari, T., Tuominen, J., Ludvigsen, H., Petersen, J., Sørensen, T., Hansen, T., and Simonsen, H., "Gas sensing using air-guiding photonic bandgap fibers," *Opt. Express* **12**(17), 4080–4087 (2004).

[15] Jha, R., Villatoro, J., Badenes, G., and Pruneri, V., "Refractometry based on a photonic crystal fiber interferometer," *Opt. Lett.* **34**(5), 617–619 (2009).

[16] Nakazawa, M., Kasai, K., and Yoshida, M., "C2h2 absolutely optical frequency-stabilized and 40 ghz repetition-rate-stabilized, regeneratively mode-locked picosecond erbium fiber laser at 1.53 μm," *Opt. Lett.* **33**(22), 2641–2643 (2008).
[17] Thapa, R., Knabe, K., Faheem, M., Naweed, A., Weaver, O. L., and Corwin, K. L., "Saturated absorption spectroscopy of acetylene gas inside large-core photonic bandgap fiber," *Opt. Lett.* **31**(16), 2489–2491 (2006).
[18] Mortensen, N. A. and Xiao, S., "Slow-light enhancement of beer-lambert-bouguer absorption," *Applied Physics Letters* **90**(14), 141108 (2007).